

# Coamoeba and mirror symmetry

(Joint work with Masahito Yamazaki)

大阪大学大学院理学研究科 植田 一石 (Kazushi Ueda)  
Graduate School of Science,  
Osaka University

## 1 Introduction

We report on our attempt to formulate an algorithm to associate a bipartite graph on a torus called a *brane tiling* to a lattice polygon, introduced by physicists Hanany and Vegh [4]. We also discuss its relation with coamoebas following Feng, He, Kenaway and Vafa [2].

A *lattice polygon* is a convex hull of a finite subset of  $\mathbb{Z}^2$  in  $\mathbb{R}^2$ . We always assume that the origin  $0 \in \mathbb{R}^2$  is in its interior. To a lattice polygon  $\Delta$ , one can associate a triangulated category of geometric origin in two different ways.

- (A) Take a Laurent polynomial  $W \in \mathbb{C}[x^{\pm 1}, y^{\pm 1}]$  whose Newton polygon coincides with  $\Delta$ . Consider the derived category  $D^b \mathfrak{Fuk}^{\rightarrow} W$  of the directed Fukaya category of  $W$ .
- (B) Take the toric Fano surface (or stack, to be more precise)  $X_{\Delta}$  associated to  $\Delta$ . Consider the derived category  $D^b \text{coh } X_{\Delta}$  of coherent sheaves on  $X_{\Delta}$ .

The directed Fukaya category of a holomorphic function is an  $A_{\infty}$ -category whose set of objects is a distinguished basis of vanishing cycles and whose spaces of morphisms are Lagrangian intersection Floer complexes. It is defined by Seidel [7] following an idea of Kontsevich [6]. An  $A_{\infty}$ -category is a generalization of a category where the spaces of morphisms are not only vector spaces but complexes of vector spaces, and the composition of morphisms are not necessarily associative but satisfy complicated compatibility conditions which ensure the associativity at the level of cohomologies. Although the directed Fukaya category  $\mathfrak{Fuk}^{\rightarrow} W$  depends on the choice of a distinguished basis of vanishing cycles, its derived category  $D^b \mathfrak{Fuk}^{\rightarrow} W$  is known to be independent of this choice by Seidel [7]. Note that  $D^b \mathfrak{Fuk}^{\rightarrow} W$  does not depend on the choice of a general Laurent polynomial whose Newton polygon coincides with  $\Delta$ , since Floer cohomologies are symplectic invariants and do not depend on the complex structure.

The toric Fano stack associated to  $\Delta$  is defined as follows: Let  $\{v_i\}_{i=1}^N$  be the set of vertices of  $\Delta$  numbered clockwise and  $K \subset (\mathbb{C}^{\times})^N$  be the kernel of the map

$$\varphi \otimes_{\mathbb{Z}} \mathbb{C}^{\times} : (\mathbb{C}^{\times})^N \rightarrow (\mathbb{C}^{\times})^2,$$

where  $\varphi : \mathbb{Z}^N \rightarrow \mathbb{Z}^2$  is a homomorphism sending the  $i$ -th coordinate vector  $e_i \in \mathbb{Z}^N$  to  $v_i$ . Put  $U = \{(x_1, x_2, x_3) \in \mathbb{C}^3 \mid (x_1, x_2, x_3) \neq (0, 0, 0)\}$  if  $N = 3$  and  $U = \{(x_i)_{i=1}^N \in$

$\mathbb{C}^n \setminus \{(x_i, x_j) \neq (0, 0) \text{ if } |i - j| > 1\}$  if  $N \geq 4$ . Then  $X_\Delta$  is the quotient stack

$$X_\Delta = [U/K]$$

of  $U$  by the natural action

$$\begin{array}{ccc} K & \curvearrowright & U & \rightarrow & U \\ \Downarrow & & \Downarrow & & \Downarrow \\ (\alpha_1, \dots, \alpha_N) & : & (x_1, \dots, x_N) & \mapsto & (\alpha_1 x_1, \dots, \alpha_N x_N) \end{array}$$

of  $K$ .

The following conjecture is due to Kontsevich [5, 6]:

**Conjecture 1 (homological mirror symmetry).** *There exists an equivalence*

$$D^b \text{coh } X_\Delta \cong D^b \mathfrak{Fuk}^\rightarrow W$$

of triangulated categories.

Hanany and Vegh [4] introduced another way to associate a triangulated category to a lattice polygon:

- (C) Take a *brane tiling* associated to  $\Delta$ , which encodes the information of a quiver  $\Gamma^\rightarrow$  with relations. Consider the derived category  $D^b \text{mod } \mathbb{C}\Gamma^\rightarrow$  of representations of this quiver.

Hanany, Herzog and Vegh [3] proposed a method to associate a sequence  $(E_1, \dots, E_N)$  of line bundles on  $X_\Delta$ , which conjecturally gives a full strong exceptional collection in  $D^b \text{coh } X_\Delta$  whose total morphism algebra is isomorphic to the path algebra of the quiver with relations obtained from  $\Delta$  through the algorithm of Hanany and Vegh;

$$\bigoplus_{i,j=1}^N \text{Hom}(E_i, E_j) \cong \mathbb{C}\Gamma^\rightarrow.$$

This conjecture, together with a theorem of Bondal [1, Theorem 6.2], implies the equivalence

$$D^b \text{coh } X_\Delta \cong D^b \text{mod } \mathbb{C}\Gamma^\rightarrow.$$

On the other hand, Feng, He, Kennaway, and Vafa [2] conjectured a relation between the brane tiling and geometry of vanishing cycles of  $W$ , which implies the equivalence

$$D^b \mathfrak{Fuk}^\rightarrow W \cong D^b \text{mod } \mathbb{C}\Gamma^\rightarrow.$$

We have shown these conjectures when  $X_\Delta$  is a toric orbifold of a toric del Pezzo surface, from which homological mirror symmetry in this case follows as a corollary [9].

## 2 The algorithm of Hanany and Vegh

### 2.1 Basic definitions

Let  $T = \mathbb{R}^2 / \mathbb{Z}^2$  be a real two-torus equipped with an orientation. A *bipartite graph* on  $T$  consists of

- a set  $B \subset T$  of black vertices,
- a set  $W \subset T$  of white vertices, and
- a set  $E$  of edges, consisting of embedded intervals  $e$  on  $T$  such that one boundary of  $e$  belongs to  $B$  and the other boundary belongs to  $W$ . We assume that two edges intersect only at the boundaries.

A *quiver* consists of

- a set  $V$  of vertices,
- a set  $A$  of arrows, and
- two maps  $s, t : A \rightarrow V$  from  $A$  to  $V$ .

For an arrow  $a \in A$ ,  $s(a)$  and  $t(a)$  are said to be the *source* and the *target* of  $a$  respectively. A *path* on a quiver is an ordered set of arrows  $(a_n, a_{n-1}, \dots, a_1)$  such that  $s(a_{i+1}) = t(a_i)$  for  $i = 1, \dots, n-1$ . We also allow for a path of length zero, starting and ending at the same vertex. The *path algebra*  $\mathbb{C}Q$  of a quiver  $Q = (V, A, s, t)$  is the algebra spanned by the set of paths as a vector space, and the multiplication is defined by the concatenation of paths;

$$(b_m, \dots, b_1) \cdot (a_n, \dots, a_1) = \begin{cases} (b_m, \dots, b_1, a_n, \dots, a_1) & s(b_1) = t(a_n), \\ 0 & \text{otherwise.} \end{cases}$$

A *quiver with relations* is a pair of a quiver and a two-sided ideal  $\mathcal{I}$  of its path algebra. For a quiver  $\Gamma = (Q, \mathcal{I})$  with relations, its path algebra  $\mathbb{C}\Gamma$  is defined as the quotient algebra  $\mathbb{C}Q/\mathcal{I}$ .

For a choice of an order  $<$  on the set  $V$  of vertices, the *directed subquiver*  $Q^\rightarrow$  is obtained from  $Q$  by eliminating the arrows  $a \in A$  satisfying  $s(a) > t(a)$ . The path algebra  $\mathbb{C}Q^\rightarrow$  is a subalgebra of  $\mathbb{C}Q$ , and an ideal  $\mathcal{I}$  of  $\mathbb{C}Q$  induces an ideal  $\mathcal{I}^\rightarrow = \mathcal{I} \cap \mathbb{C}Q^\rightarrow$  of  $\mathbb{C}Q^\rightarrow$ .

### 2.2 Admissible families

Let  $\Delta \subset \mathbb{R}^2$  be a lattice polygon, i.e., the convex hull of a finite subset of  $\mathbb{Z}^2$ . An *edge* of  $\Delta$  is a connected component of the boundary  $\partial\Delta \setminus (\partial\Delta \cap \mathbb{Z}^2)$  of  $\Delta$  minus its lattice points. For example, both the convex hull  $\Delta_2$  of  $(-1, 0)$ ,  $(1, 0)$  and  $(0, 1)$  shown in Figure 1 and the convex hull  $\Delta_4$  of  $(1, 0)$ ,  $(0, 1)$ ,  $(-1, 0)$  and  $(-1, -1)$  shown in Figure 2 have four edges.

For each edge  $a$  of  $\Delta$ , draw an oriented line  $L_a$  on  $T$  in the direction of its primitive outward normal vector. Since the choice of  $L_a$  is unique up to translations, the set  $\text{Conf}(\Delta)$  of families  $\{L_a\}_a$  of oriented lines is a torus  $(S^1)^n$ , where  $n$  is the number of edges of  $\Delta$ . Let  $S$  be the set of families  $\{L_a\}_a$  such that more than two lines meet at one point. We will restrict ourselves to families  $\{L_a\}_a$  from the complement  $\text{Conf}(\Delta) \setminus S$  henceforth, i.e., we assume that no three lines meet at one point. A family  $\{L_a\}_a$  divides  $T$  into a finite number of polygons  $\{P_i\}_{i=1}^m$ . A polygon  $P_i$  is called *white* if the orientations of  $L_a \cap P_i$  induced from those of  $L_a$  and  $P_i$  coincide for all the edges  $a$ , and *black* if they are opposite for all the edges. A connected component of  $(\cup_a L_a) \setminus (\cup_{a,b} (L_a \cap L_b))$  can bound at most one colored polygon, and the family  $\{L_a\}_a$  is called *admissible* if it always does.

The set  $\pi_0(\text{Conf}(\Delta) \setminus S)$  classifies families of oriented lines up to small perturbations which do not change the combinatorial structure. The fundamental question is the following:

**Problem 2.**

1. *Is there an admissible family of oriented lines for any lattice polygon  $\Delta$ ?*
2. *If there is one, then is the class of admissible families in  $\pi_0(\text{Conf}(\Delta) \setminus S)$  unique?*

We know the answer when  $X_\Delta$  is a toric del Pezzo surface by a brute-force case-by-case analysis: When  $X_\Delta$  is  $\mathbb{P}^2$ ,  $\mathbb{P}^1 \times \mathbb{P}^1$ , or  $\mathbb{P}^2$  blown-up at one point, then there is a unique class of admissible family. When  $X_\Delta$  is  $\mathbb{P}^2$  blown-up at two or three points, then there are two classes of admissible families related by a reflection, so that the resulting quivers with relations are isomorphic.

As an example, consider families of oriented lines for the triangle  $\Delta_2$  in Figure 1. There are two combinatorially distinct ways shown in Figure 3 and Figure 4 to arrange four lines in the directions of outward normal vectors of the edges of  $\Delta_2$ . In Figure 3, all the connected components of  $(\cup_a L_a) \setminus (\cup_{a,b} (L_a \cap L_b))$  bound colored polygons, whereas in Figure 4, the connected components of  $(\cup_a L_a) \setminus (\cup_{a,b} (L_a \cap L_b))$  drawn in dotted lines do not bound any colored polygon. Hence the polygon  $\Delta_2$  in Figure 1 has a unique class of admissible families. In the same way, one can show that the quadrilateral  $\Delta_4$  in Figure 2 has a unique class of admissible families shown in Figure 7.

### 2.3 Brane tilings and quivers

To an admissible family  $\{L_a\}_a$ , one associates a bipartite graph on  $T$  called the *brane tiling* as follows; the set  $W$  of white vertices is the set of the centers of gravities of white polygons, and the set  $B$  of black vertices is the set of the centers of gravities of black polygons. For a pair of colored polygons sharing a vertex, their centers of gravities are connected by a straight line segment. For example, Figure 5 shows the brane tiling associated with the admissible family in Figure 3, and Figure 8 shows the brane tiling associated with the admissible family in Figure 7.

A brane tiling  $(B, W, E)$  encodes the information of a quiver  $\Gamma = (V, A, s, t, \mathcal{I})$  with relations in the following way: The set  $V$  of vertices is the set of connected components

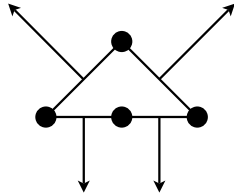


Figure 1: A triangle  $\Delta_2$

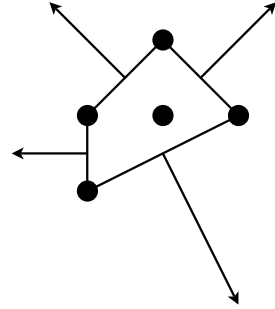


Figure 2: A quadrilateral  $\Delta_4$

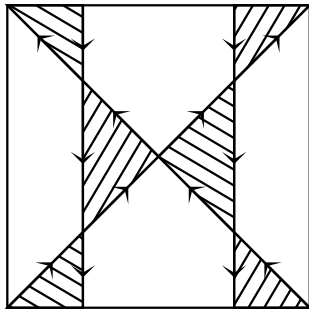


Figure 3: The admissible family

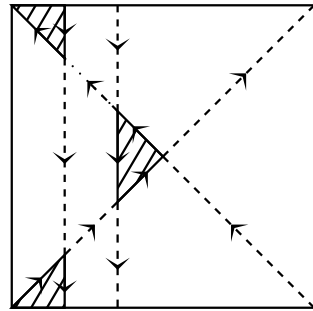


Figure 4: The non-admissible family

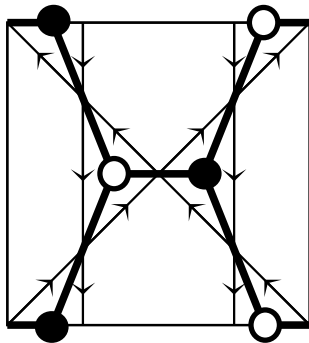


Figure 5: The brane tiling

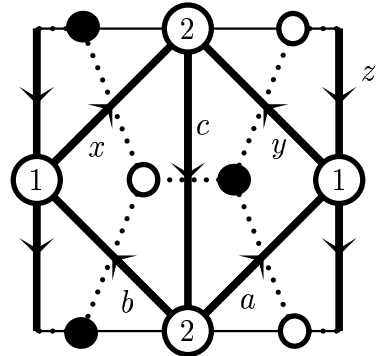


Figure 6: The quiver

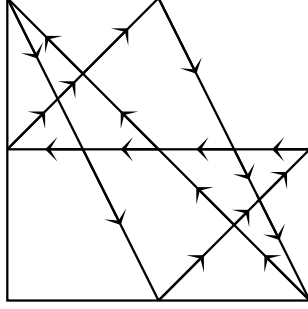


Figure 7: The unique admissible family for  $\Delta_4$

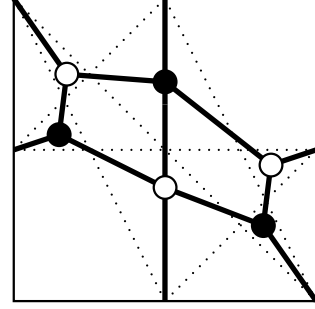


Figure 8: The brane tiling

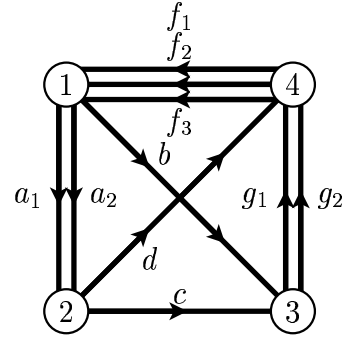
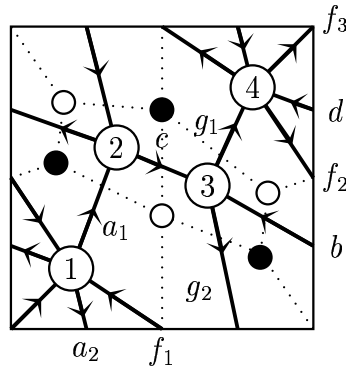


Figure 9: The quiver  $\Gamma_4$

of the complement  $T \setminus (\bigcup_{e \in E} e)$ , and the set  $A$  of arrows is the set  $E$  of edges of the graph. The directions of the arrows are determined by the colors of the vertices of the graph, so that the white vertex  $w \in W$  is on the right of the arrow. In other words, the quiver is the dual graph of the brane tiling equipped with an orientation given by rotating the white-to-black flow on the edges of the brane tiling by minus 90 degrees. For example, Figure 6 and Figure 9 show the quivers associated to the brane tilings in Figure 5 and Figure 8 respectively.

The relations of the quiver are described as follows: For an arrow  $a \in A$ , there exist two paths  $p_+(a)$  and  $p_-(a)$  from  $t(a)$  to  $s(a)$ , the former going around the white vertex connected to  $a \in E = A$  clockwise and the latter going around the black vertex connected to  $a$  counterclockwise. Then the ideal  $\mathcal{I}$  of the path algebra is generated by  $p_+(a) - p_-(a)$  for all  $a \in A$ .

For example, the ideal of relations for the quiver in Figure 6 is given by

$$(yz - cy, cx - xz, xb - ya, bc - zb, za - ac, ay - bx),$$

whereas that for the quiver in Figure 9 is given by

$$(f_1g_2c - f_2d, f_3d - f_1g_1c, f_2g_1 - f_3g_2, a_1f_1g_2 - a_2f_1g_1, \\ a_2f_3 - a_1f_2, g_2ca_1 - g_1ca_2, g_1b - da_1, da_2 - g_2b).$$

The last step in the algorithm of Hanany and Vegh is the choice of an order on the set of vertices of the quiver. This involves the choice of an *internal perfect matching*

of the brane tiling. We refer the reader to [9, section 4] for the description of this step. This choice of an order corresponds to the choice of a foundation of a helix in  $D^b \text{coh } X_\Delta$ , and to the choice of an order in the distinguished basis of vanishing cycles in  $D^b \mathfrak{Fut}^\rightarrow W$ . The quiver  $\Gamma^\rightarrow$  appearing in section 1 is the directed subquiver of  $\Gamma$  with respect to this order.

### 3 Coamoebas and Newton polygons

Here we discuss the relation between Newton polygons and asymptotic behaviors of coamoebas. The *coamoeba* of an algebraic subvariety of a torus  $(\mathbb{C}^\times)^n$  is defined by Passare and Tsikh as its image by the argument map

$$\begin{aligned} (\mathbb{C}^\times)^n &\xrightarrow{\quad \Psi \quad} (\mathbb{R}/\mathbb{Z})^n \\ (x_1, \dots, x_n) &\mapsto \frac{1}{2\pi}(\arg(x_1), \dots, \arg(x_n)). \end{aligned} \tag{1}$$

Here  $n$  is a natural number. Consider the case when  $n = 2$ . For a Laurent polynomial

$$W(x, y) = \sum_{(i,j) \in \mathbb{Z}^2} a_{ij} x^i y^j$$

in two variables, its *Newton polygon* is defined as the convex hull

$$\Delta = \text{Conv}\{(i, j) \in \mathbb{Z}^2 \mid a_{ij} \neq 0\} \subset \mathbb{R}^2.$$

For an edge  $e$  of  $\Delta$ , let  $(n(e), m(e)) \in \mathbb{Z}^2$  be the primitive outward normal vector of  $e$  and  $l(e)$  be the integer such that the defining equation for the edge  $e$  is

$$n(e)i + m(e)j = l(e).$$

The *leading term* of  $W$  with respect to the edge  $e$  is defined by

$$W_e(x, y) = \sum_{n(e)i + m(e)j = l(e)} a_{ij} x^i y^j.$$

This is indeed the leading term if we put

$$(x, y) = (r^{n(e)}u, r^{m(e)}v), \quad r \in \mathbb{R} \text{ and } u, v \in \mathbb{C}^\times$$

and take the  $r \rightarrow \infty$  limit;

$$P(r^{n(e)}u, r^{m(e)}v) = r^{l(e)}W_e(u, v) + O(r^{l(e)-1}).$$

Now assume that for an edge  $e$ , the leading term  $W_e(x, y)$  is a binomial

$$W_e(x, y) = \mathbf{e}(\alpha_1)x^{i_1}y^{j_1} + \mathbf{e}(\alpha_2)x^{i_2}y^{j_2},$$

where  $\alpha_1, \alpha_2 \in \mathbb{R}/\mathbb{Z}$ ,  $(i_1, j_1), (i_2, j_2) \in \mathbb{Z}^2$  and  $\mathbf{e}(\alpha_i) = \exp(2\pi\sqrt{-1}\alpha_i)$  for  $i = 1, 2$ . Put

$$(x, y) = (r^{n(e)}\mathbf{e}(\theta), r^{m(e)}\mathbf{e}(\phi)).$$

Then the leading behavior of  $W$  as  $r \rightarrow \infty$  is given by

$$r^{l(e)}W_e(\mathbf{e}(\theta), \mathbf{e}(\phi)) = r^{l(e)}\{\mathbf{e}(\alpha_1 + i_1\theta + j_1\phi) + \mathbf{e}(\alpha_2 + i_2\theta + j_2\phi)\}. \quad (2)$$

Hence the coamoeba of  $W^{-1}(0)$  asymptotes in this limit to the line

$$(\alpha_2 - \alpha_1) + (i_2 - i_1)\theta + (j_2 - j_1)\phi + \frac{1}{2} = 0 \pmod{\mathbb{Z}}$$

on the torus  $T = (\mathbb{R}/\mathbb{Z})^2$ . This line will be called an *asymptotic boundary* of the coamoeba of  $W^{-1}(0)$ .

The asymptotic boundary has a natural orientation coming from the outward normal vector of the edge of  $\Delta$ . To understand the role of this orientation, take a pair of adjacent edges  $e$  and  $e'$  of  $\Delta$  as in Figure 10 and consider the behavior of the coamoeba of  $W^{-1}(0)$  near the intersection of asymptotic boundaries corresponding to  $e$  and  $e'$ . Assume that the leading terms corresponding to  $e$  and  $e'$  are binomials

$$\begin{aligned} W_e(x, y) &= \mathbf{e}(\alpha)x^{i_1}y^{j_1} + \mathbf{e}(\beta)x^{i_2}y^{j_2}, \\ W_{e'}(x, y) &= \mathbf{e}(\beta)x^{i_2}y^{j_2} + \mathbf{e}(\gamma)x^{i_3}y^{j_3} \end{aligned}$$

for some  $\alpha, \beta, \gamma \in \mathbb{R}/\mathbb{Z}$  and  $(i_1, j_1), (i_2, j_2), (i_3, j_3) \in \mathbb{Z}^2$ . Put

$$W_{ee'}(x, y) = \mathbf{e}(\alpha)x^{i_1}y^{j_1} + \mathbf{e}(\beta)x^{i_2}y^{j_2} + \mathbf{e}(\beta)x^{i_3}y^{j_3}.$$

Assume further that all the coefficients of  $W$  corresponding to interior lattice points of the Newton polygon of  $W_{ee'}$  vanish. Then  $W_{ee'}$  is the sum of the leading term and the subleading term of  $W$  as one puts

$$(x, y) = (r^{-n(e'')}u, r^{-m(e'')}v), \quad r \in \mathbb{R}^{>0} \text{ and } u, v \in \mathbb{C}^\times,$$

and take the  $r \rightarrow \infty$  limit. Here,  $(n(e''), m(e'')) \in \mathbb{Z}^2$  is the primitive outward normal vector of the edge  $e''$  of the Newton polygon of  $W_{ee'}$  shown in Figure 10. The coamoeba for the sum of three monomials has been analyzed in [8]; the asymptotic boundaries coincide with the actual boundaries of the coamoeba, and the orientations on the asymptotic boundaries determine which side of the boundary belongs to the coamoeba. Hence the orientations of asymptotic boundaries determine the leading behavior of the coamoeba near the intersections of asymptotic boundaries as in Figure 11.

## 4 Coamoeba and vanishing cycles

Here we discuss the vanishing cycles of

$$W(x, y) = x + y - \frac{1}{x} + \frac{1}{xy}$$



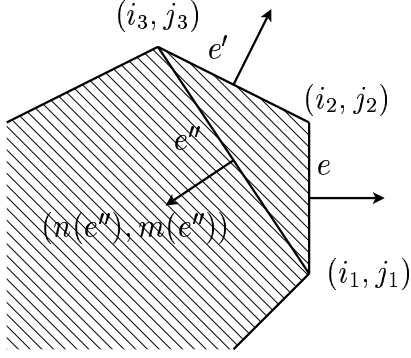


Figure 10: A pair of adjacent edges of the coamoeba near an intersection of asymptotic boundaries.

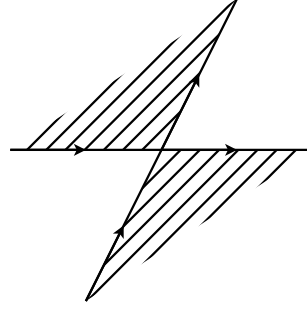


Figure 11: The leading behavior of the coamoeba near an intersection of asymptotic boundaries.

and their images under the argument map. The Newton polygon of  $W$  is the quadrilateral  $\Delta_4$  shown in Figure 2. The holomorphic map  $W$  has four critical points. Take the origin as the base point and let  $(c_i)_{i=1}^4$  be the distinguished set of vanishing paths, defined as the straight line segments from the origin to the critical values.

The asymptotic boundary of the coamoeba of  $W^{-1}(0)$  is shown in Figure 12, which coincides with the unique admissible family of oriented lines shown in Figure 7. Figure 13 shows a schematic picture of the actual coamoeba. To study the image of the vanishing cycles by the argument map, we cut the coamoeba into pieces along the bold lines in Figure 14. They cut  $W^{-1}(0)$  into the union of two quadrilaterals and four triangles, glued along ten edges. By gluing these pieces, one obtains an elliptic curve minus four points shown in Figure 15. It turns out that the vanishing cycles on  $W^{-1}(0)$  looks as in Figure 16, whose images by the argument map encircles the holes in the coamoeba as shown in Figure 17.

The strategy for the proof of the equivalence

$$D^b \mathfrak{Fuk}^{\rightarrow} W \cong D^b \text{mod CT}$$

is summarized in Table 1. The vertices of the brane tiling correspond to the disks,

graph	$W^{-1}(0)$	quiver
vertex	disk	relation
color	orientation	sign
face	vanishing cycle	vertex
edge	intersection	arrow

Table 1: A dictionary

which are glued together to form the regular fiber  $W^{-1}(0)$ . The color of a vertex determines whether this gluing procedure preserves or reverses the cyclic order on the set of edges connected to the vertex. The set of faces of the brane tiling corresponds to the set of vanishing cycles, and the set of edges are in bijection with the set of intersection points of vanishing cycles under this correspondence. The set of vanishing cycles is the set of objects in the directed Fukaya category  $\mathfrak{Fuk}^{\rightarrow} W$ , and the set of their

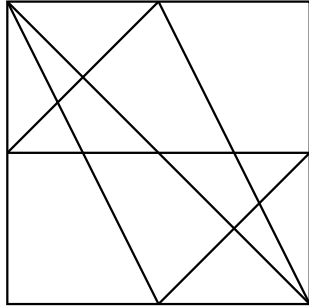


Figure 12: The asymptotic boundary

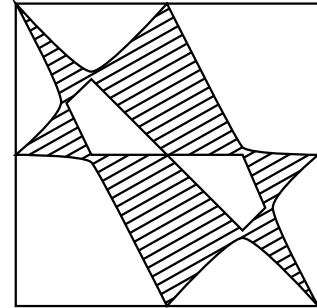


Figure 13: The actual coamoeba

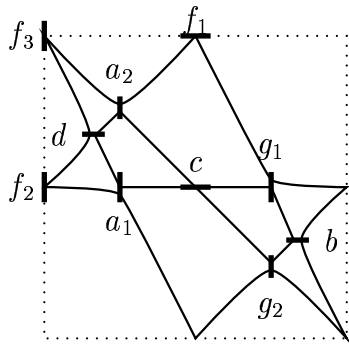


Figure 14: Cutting the coamoeba into pieces

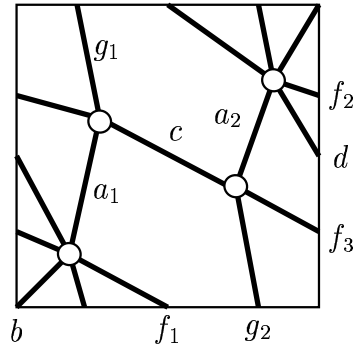


Figure 15: The glued surface

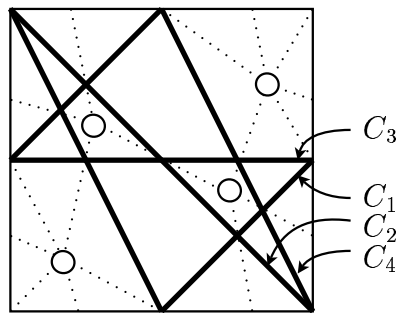


Figure 16: The vanishing cycles

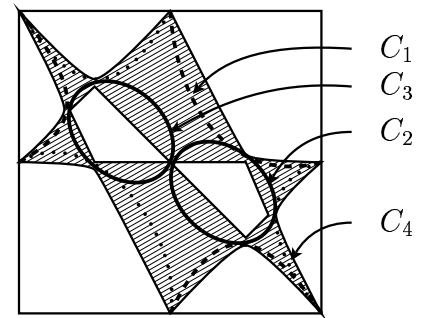


Figure 17: Vanishing cycles on the coamoeba

intersection points spans the spaces of morphisms. To make a quiver with relations which is derived-equivalent to  $\mathfrak{Fuk}^{\rightarrow} W$ , we assign a vertice to each object of  $\mathfrak{Fuk}^{\rightarrow} W$  and an arrow to each basis of the spaces of morphisms. The relations in the quiver come from  $A_{\infty}$ -operations in  $\mathfrak{Fuk}^{\rightarrow} W$ , which in turn come from holomorphic disks in  $W^{-1}(0)$  with Lagrangian boundary conditions. The color of a vertex of the brane tiling determines the sign of the contribution of the disk to the  $A_{\infty}$ -operation in  $\mathfrak{Fuk}^{\rightarrow} W$ .

## References

- [1] A. I. Bondal. Representations of associative algebras and coherent sheaves. *Izv. Akad. Nauk SSSR Ser. Mat.*, 53(1):25–44, 1989.
- [2] Bo Feng, Yang-Hui He, Kristian D. Kennaway, and Cumrun Vafa. Dimer models from mirror symmetry and quivering amoebae. hep-th/0511287, 2005.
- [3] Amihay Hanany, Christopher P. Herzog, and David Vegh. Brane tilings and exceptional collections. hep-th/0602041, 2006.
- [4] Amihay Hanany and David Vegh. Quivers, tilings, branes and rhombi. hep-th/0511063, 2005.
- [5] Maxim Kontsevich. Homological algebra of mirror symmetry. In *Proceedings of the International Congress of Mathematicians, Vol. 1, 2 (Zürich, 1994)*, pages 120–139, Basel, 1995. Birkhäuser.
- [6] Maxim Kontsevich. Lectures at ENS Paris, spring 1998. set of notes taken by J. Bellaïche, J.-F. Dat, I. Martin, G. Rachinet and H. Randriambololona, 1998.
- [7] Paul Seidel. Vanishing cycles and mutation. In *European Congress of Mathematics, Vol. II (Barcelona, 2000)*, volume 202 of *Progr. Math.*, pages 65–85. Birkhäuser, Basel, 2001.
- [8] Kazushi Ueda and Masahito Yamazaki. A note on brane tilings and McKay quivers. math.AG/0605780, 2006.
- [9] Kazushi Ueda and Masahito Yamazaki. Homological mirror symmetry for toric orbifolds of toric del Pezzo surfaces. math.AG/0703267, 2007.